Nanopatterning of photonic crystals with a photocurable silica–titania organic–inorganic hybrid material by a UV-based nanoimprint technique

Woo-Soo Kim,[a] Keun Byoung Yoon[b] and Byeong-Soo Bae*[a]

Received 7th July 2005, Accepted 19th August 2005
First published as an Advance Article on the web 13th September 2005
DOI: 10.1039/b509622g

UV patternable high refractive index inorganic–organic hybrid materials prepared by sol–gel process can be nanoimprinted in order to get photonic crystal nanopatterns. Non-hydrolytic sol–gel process can make a UV curable and relatively high refractive index hybrid material, which can be cured without a significant shrinkage for nanoimprinting. Sol–gel process of heterogeneously functionalized silicon alkoxides can make the organically modified inorganic Si–O–Ti network very well. The UV-based nanoimprint technique utilizes transparent templates and UV curable high refractive index materials to allow pattern replication at room temperature and very low pressure. UV-based nanoimprint technique is an efficient way to fabricate this sort of polymeric photonic crystal nanostructures.

Introduction

Dielectric thin films with periodic nanopatterns, known as photonic crystals (PC), can exhibit many interesting optical properties such as photonic band gap,[1,2] *i.e.*, the frequency range where an electromagnetic wave cannot propagate through the films. Thus, photonic crystals are expected to be useful in the implementation of new functional optical devices and optical properties, such as bent waveguides, superprism phenomenon,[3,4] self-collimated beam propagation,[5] form birefringence,[6] and so on. Most successful PC structures have been fabricated in semiconductors,[7–9] since semiconductor processing techniques, such as electron beam lithography, provide the most advanced tools for the fabrication of nanometric structures. Nanopatterning of photonic crystals has been conventionally achieved by electron beam lithography and dry-etching methods such as inductively coupled plasma (ICP) or reactive ion etching (RIE) techniques. However, these techniques are expensive and time-consuming. For these reasons, faster and cheaper lithographic techniques are desirable, especially for application to organic semiconductors. Hence, the nanofabrication of thin films with periodic patterns using a parallel and low cost technique such as nanoimprinting lithography (NIL) has recently attracted considerable attention.[10] Nanoimprint lithography has been demonstrated to be a high volume and cost-effective patterning technique with sub-10 nm resolution and has great potential as a candidate for next generation lithography.[11,12] In nanoimprint lithography, a mold with nanoscale features is pressed into a thin resist film, deforming the shape of the film according to the features of the mold and forming a relief pattern in the film. UV-based nanoimprint lithography has been developed as an alternative to the hot embossing technique.[13,14] Nanoimprint technique is of interest for single step processes, which have to deliver a surface roughness below the wavelength of the light, for example in PC structures.[15] Recent progress in the molecular engineering of polymers has stimulated the development of organic photonics.[16] However, most polymer photonic crystals have incomplete in-plane photonic band gaps. Thus, they are not suitable for the implementation of waveguides and cavities, which play key roles in photonic band gap functional devices, due to their low refractive index contrast.[17–19]

In the present study, we report on experimental results of UV-based nanoimprinted photonic crystal structure and synthesis of photocurable high refractive index materials. We have synthesized a resin-type high refractive index material that can be curable by low energy UV light. This allows investigation of a high-resolution printing technique based on transferring a pattern from an elastomeric mold to a solid substrate by the UV-based nanoimprinting technique. This is an attempt to enhance the accuracy of classical printing to a precision comparable with optical lithography, thereby creating a low-cost, high-resolution patterning process. This aim of this study is to provide a cost-efficient technique based on UV nanoimprint technology and high refractive index materials for the fabrication of polymeric photonic crystal nanostructures. The high refractive index materials are organic–inorganic hybrid materials (hybrimers[20,21]), which are synthesized by a non-hydrolytic sol–gel process.

Thus, the non-hydrolytic sol–gel process differs from the conventional hydrolytic sol–gel process in the synthesis of polysiloxane resin without solvent. Hybrimers synthesized by a non-hydrolytic sol–gel process are suitable for soft lithographic applications and thus this process can be employed to obtain a crack-free patterned structure and little volume contraction.[22]

Experimental

Preparation of UV curable silica–titania hybrimer resin

3-(Trimethoxysilyl)propyl methacrylate (MPTMS, Aldrich), diphenylsilanediol (DPSD, TCI), and titanium ethoxide

[a]*Laboratory of Optical Materials and Coating (LOMC), Department of Materials Science and Engineering, Korea Advanced Institute of Science and Technology (KAIST), 373-1 Guseong-dong, Yuseong-gu, Daejeon, Republic of Korea. E-mail: bsbae@kaist.ac.kr*
[b]*Department of Polymer Science & Engineering, Kyungpook National University, 1370 Sankyug-dong, Buk-gu, Daegu 702-701, Korea*

($Ti(OC_2H_5)_4$ Aldrich) were used as starting molecules, and barium hydroxide monohydrate ($Ba(OH)_2{\cdot}H_2O$, Aldrich) was used as a catalyst to promote the condensation reaction among the precursors. First, a homogeneous titanium ethoxide solution was prepared by chelating titanium ethoxide ($Ti(OC_2H_5)_4$, Aldrich) with ethyl acetoacetate ($CH_3COCH_2CO_2C_2H_5$, EacAc, Aldrich) in a 1 : 1 molar ratio. This chelated titanium ethoxide was stirred with MPTMS in a 1 : 1 molar ratio. Finally, DPSD was continuously added to this solution with a small amount of $Ba(OH)_2{\cdot}H_2O$ at 80 °C for 2 h to prevent self-condensation of DPSD and phase separation. Barium hydroxide monohydrate was added as about 0.1 mol% of the precursors as a catalyst. The catalyst was mixed only once in the first stage of resin preparation with MPTMS precursor. Hence, the total proportion of MPTMS, titanium ethoxide, and DPSD together was 1 : 1 : 1. The solution was kept at 80 °C for an additional 2 h for complete condensation reaction. The silanol of DPSD can be reacted with the alkoxy groups of titanium ethoxide as well as MPTMS, to form a Si–O–Si or a Si–O–Ti inorganic network. After these reactions, methanol and ethanol, which are by-products of the condensation reactions among the precursors, were extracted by vacuum heating. The solution was cooled to room temperature and filtered through a 0.45 μm size filter to remove remaining catalyst ($Ba(OH)_2{\cdot}H_2O$). Finally, we obtained a photocurable silica–titania hybrimer. Thereafter, the obtained photocurable silica–titania hybrimer resin was mixed with a photoinitiator, Irgacure369 (Ciba Geigy), which facilitates curing by UV light during the nanoimprinting step.

Preparation for UV-based nanoimprinting

The silicon master was produced by electron beam lithography and reactive ion etching using a polymethylmethacrylate (PMMA; 600 kg mol^{-1}, dissolved in ethylacetate) resist and a Cr-metal masking layer for the etching process. The exposure tool for this work was a Leica EBPG500 electron beam exposure system operated at 100 kV. The development of the resist was performed by a MIBK–IPA mixture solution. Cr was deposited on a silicon wafer as thin as 20 nm for transfer of the image onto the silicon wafer. Si etching was carried out a power of 200 W and O_2–CHF_3–SF_6 (5–40–2) pressure of 20 mTorr. The etching rate was about 40 nm min^{-1}. Following the Si etch, the remaining Cr was stripped away, thereby producing a final master. Fig. 4(A) below shows the silicon master of rods arrays fabricated using high-resolution electron beam lithography, liftoff of chrome, and O_2–CHF_3–SF_6 RIE. Near IR absorption spectra of the resins were obtained with a UV–vis–NIR spectrophotometer (Shimadzu UV-3010PC) with 1 cm path quartz cell. The scan interval was 2° through the whole measured range. The nanoimprinted patterns were investigated by means of scanning electron microscopy (Philips XL30SFEG) and atomic force microscope (SPA 400 of Seiko) microscope. During the UV curing step of nanoimprinting, the sample was cured by the UV light of a mercury lamp (365 nm wavelength) for 30 s at a UV energy of 2.5 J cm^{-2}. Finally, the sample was cured thermally at 150 °C for 3 h.

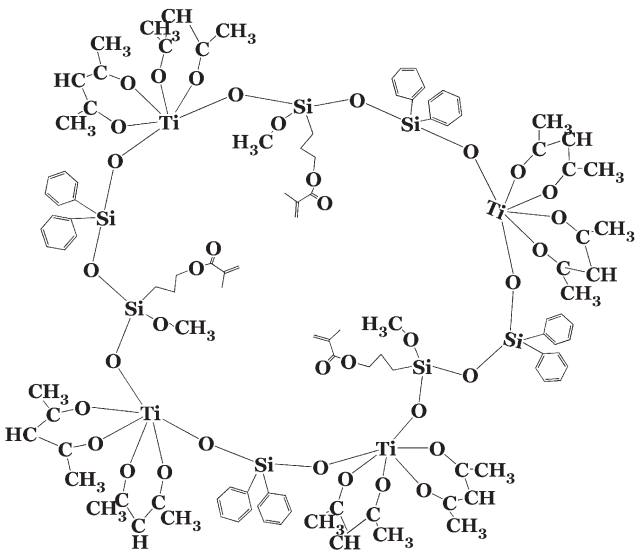

Fig. 1 Oligomer structure of methacryl silica–titania hybrimer before crosslinking.

Characterization

Refractive indices of the hybrimer films were measured using a Metricon 2010 prism coupler using light from a 0.85 μm laser diode, a 1.3 μm laser diode, and a 1.55 μm laser diode. Inorganic and organic moieties were checked by FT-IR and FT-Raman spectroscopy. X-Ray photoelectron spectroscopy (XPS) of the methacryl silica–titania hybrimer, indicating a network of inorganic Si–O–Si and Si–O–Ti bonds. The optical absorption of the methacryl silica–titania hybrimer was characterized with UV–vis–near IR spectroscopy.

Results and discussion

Characterstics of UV curable methacryl silica–titania hybrimer resin

The expected oligomer units of methacryl silica–titania hybrimer are shown in Fig. 1. Considering the several ring structures in the FT-Raman spectra of the methacryl silica–titania hybrimer (Fig. 2(a)), the expected methacryl silica–titania hybrimer resin would be a ring structured oligomer type, as shown in Fig. 1. Hexaphenyl cyclotrisiloxane, as a reference material, shows only three membered ring at 615 cm^{-1}. Because a peak of 450 cm^{-1} in the FT-Raman spectrum of the methacryl silica–titania hybrimer is shown so high, there can be multi-membered ring structures in methacryl silica–titania hybrimer, compared with the peak of hexaphenyl cyclotrisiloxane.

Fig. 2(b) shows the FT-IR spectrum of the methacryl silica–titania hybrimer before photocuring and after photocuring. At 1640 cm^{-1}, the vibrational mode of C=C stretching resulting from the methacrylic groups *appears before* photocuring the sample. UV light can convert C=C double bonds to C–C single bonds during the UV-based nanoimprinting step. This results in a solid imprinted pattern on the hybrimer. After the imprinting step with a UV dose, this peak almost disappears like the dashed peak of Fig. 2(b). Thus, the organic methacryl

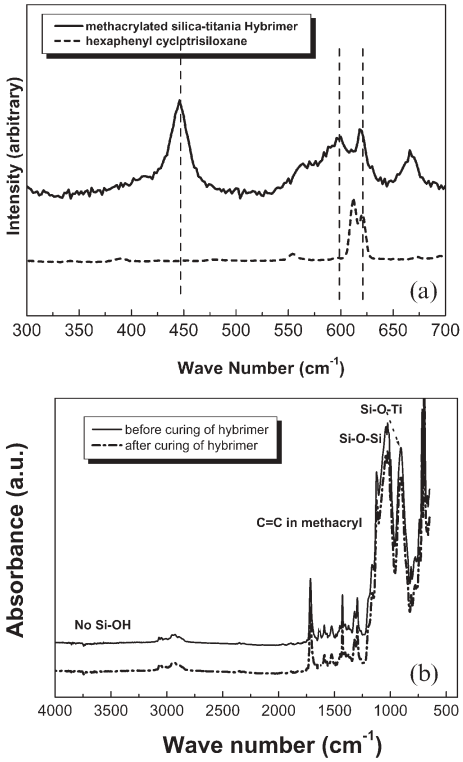

Fig. 2 FT-Raman spectra (a) and FT-IR spectra (b) of methacryl silica–titania hybrimer.

silica–titania network is cross-linked. In addition, a peak at 1720 cm^{-1} is observed. This peak is attributed to the methacrylic C=O stretching vibrational mode whereas the peak at 1590 cm^{-1} results from the aromatic C=C double bond stretching vibrational mode of the phenyl groups. Si–O–Si bond peaks appear in the range of 1000–1100 cm^{-1}. This indicates that an Si–O–Si network was formed by poly-condensation of Si–OH groups. The Si–O–Ti band of the inorganic segment is shown at 920 cm^{-1}.[23] This indicates successful bonding of the titania segment with the organic methacryl moiety. There is no absorption band around 3500 cm^{-1}, which is assigned to the Si–OH residual group of DPSD. This also shows that the network was formed well by poly-condensation of Si–OH groups of DPSD. Fig. 3 presents X-ray photoelectron spectroscopy (XPS) of the methacryl silica–titania hybrimer, indicating a portion of heterogeneous Si–O–Ti bonding with Si–O–Si bonding has occurred. The 535 eV indicates oxygen bonding energy with silicon and the lower energy bonding of 532 eV indicates heterogeneous Si–O–Ti bonding.

The optical absorption of the methacryl silica–titania hybrimer was characterized with UV–vis–near IR spectroscopy. Optical absorption *of near IR region* is one of the dominant factors considered in the propagation of light through an optically applied material. The methacryl silica–titania hybrimer shows low optical absorption *in near IR region*, because it has low Si–OH content (at 3500 nm^{-1} of Fig. 2 (b)). The absorption of the methacryl silica–titania hybrimer is 0.26 dB cm^{-1} at 850 nm, 0.18 dB cm^{-1} at 1310 nm, and 0.18 dB cm^{-1} at 1550 nm.

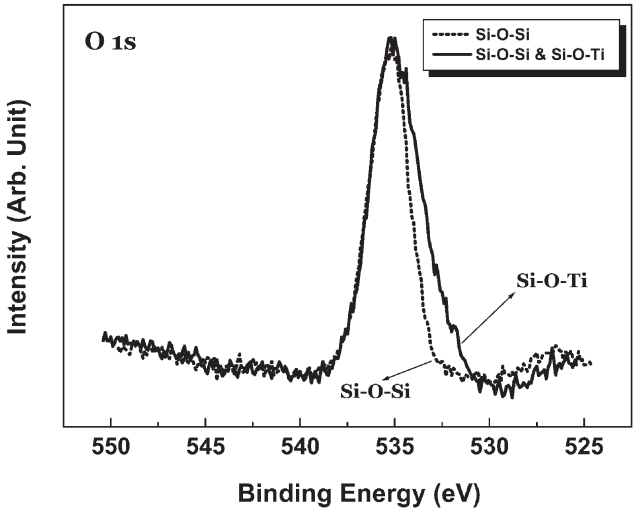

Fig. 3 Oxygen 1s XPS spectra of the methacryl silica–titania hybrimer, showing Si–O–Ti heterogeneous condensation.

The Lorenz–Lorenz equation is used for designing high refractive index materials. It shows the relationship between the refractive index and molecular structure.

$$\frac{n_D^2-1}{n_D^2+2}=\frac{[R_D]}{M}\times\rho=\frac{[R_D]}{V}$$

According to the equation, larger density (ρ), larger molecular refraction (R_D), and smaller molecular volume (V) lead to a larger refractive index (n_D). The refractive index of titania is 2.01 at 633 nm, indicating that the refractive index can be tuned with titania content. In order to prevent phase separation and to provide patternability to the resin, the ratio of Ti-containing alkoxide/Si-containing alkoxide content of methacryl silica–titania hybrimer was selected as 0.5. The refractive index of the prepared methacryl silica–titania hybrimer film is 1.623 at 633 nm.

Fabrication of photonic crystal pattern by nanoimprinting

The UV-based nanoimprint technique, as depicted in Fig. 4, utilizes transparent templates and UV curable materials to allow pattern replication at room temperature and very low pressure. Among the most recent and promising soft lithographic techniques, this method combines useful aspects of both embossing and UV-based nanoimprint techniques, using elastomeric elements and exploiting the glass transition of organic compounds to transfer the pattern. In a hot embossing technique, the master (in this case a silicon master) is placed onto a polymethylmetacrylate (PMMA) film, which is driven above the glass transition temperature T_g of the silicon substrate. The subsequent cool-down below T_g freezes the nanopattern into the PMMA and the replication can be peeled off. The replicated PMMA master can be used as a mother master for replication of a PDMS mold. Polydimethylsiloxane (PDMS), a kind of silicone rubber, is used as the mold material. The PDMS is supplied in the form of a curing agent (A) and a liquid silicon rubber base (B). We mixed A and B with a ratio of 1 : 10 and poured the mixture over the original master. After an hour of stabilization, the mixture was cured at 90 °C for 20 min. After obtaining the embossed nanopatterns,

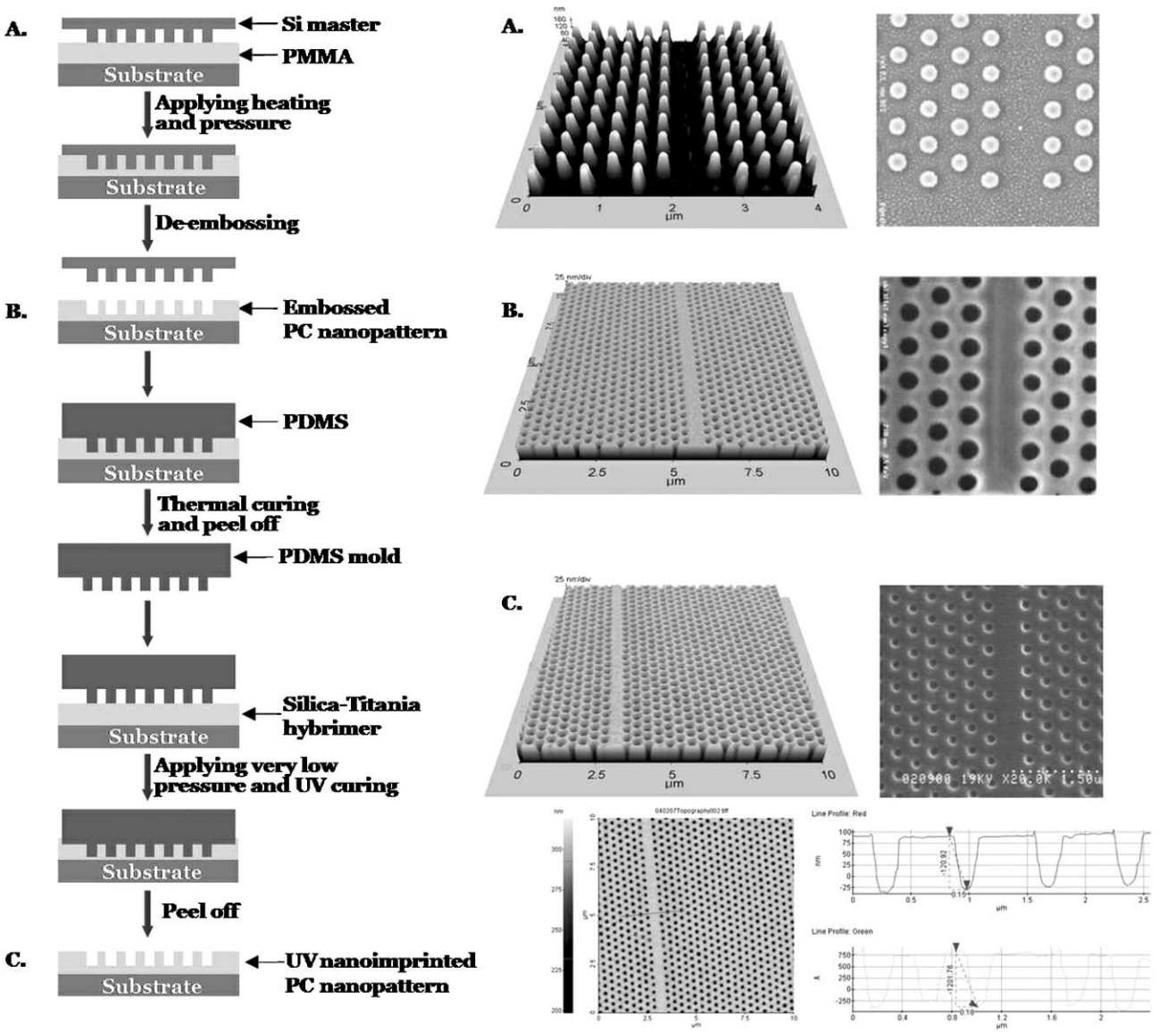

Fig. 4 Schematic diagram of the processes of UV-based nanoimprint technique and AFM and SEM images of each step: (A) silicon master of triangular circular rods array with a 100 nm diameter and 130 nm height, (B) embossed hole nanostructures with 105 nm diameter and 127 nm depth by hot embossing technique, (C) imprinted hole nanostructures with 105 nm diameter and 127 nm depth by UV-based nanoimprint technique.

we could fabricate the PDMS mold by the transfer molding technique. The cured PDMS rubber does not adhere to the embossed nanopatterns and is flexible. As such, it can be easily peeled from the embossed nanopatterns. The PDMS mold has the complementary shape of nanopatterns of the original master and embossed nanopattens. The resulting mold is shown in Fig. 4. In replicating nanopatterns of the elastomeric mold to the UV curable materials, we follow the UV-based nanoimprint process of placing the PDMS stamp on the silicon wafer. The methacryl silica–titania hybrimer was used for the UV-based nanoimprint of photonic crystal. The photonic crystal nanostructure was fabricated by a nanoimprint system (Obducat, Sweden). A 300 nm PMMA (25 kg mol^{-1}, dissolved in ethylacetate) film on the silicon substrate was placed at the bottom of the embossing plate and the silicon master was placed above the PMMA film on the silicon substrate. The embossing was carried out by applying heat and pressure.[24,25] The embossing plate was heated to 150 °C and 30 bar of pressure was then applied to the silicon master and the PMMA film on the silicon substrate with 1 min of holding time. The de-embossing temperature was 75 °C and the total processing time was approximately 5 min. Fig. 4(B) shows atomic force microscopy (AFM) images of the hot embossed photonic crystal nanostructures. In Fig. 4(B), embossed triangular circular holes in PMMA appear to conform to the master. The dark centers of the holes correspond to the embossed narrow shafts of the circular rods on the silicon master. Using the silicon master, holes having 105 nm diameter and 405 nm pitch were embossed in the PMMA film on the silicon substrate. In Fig. 4(B), we cannot observe sticking or peel-off between the polymer and silicon master. The photonic crystal nanostructures on the master are undamaged by the hot embossing process. The original patterns of the master are effectively replicated to the polymer thin film by a hot

embossing technique. We have developed a UV-based nanoimprint technique to replicate a photonic crystal nanostructure on a silicon substrate with PDMS mold. In the UV-based nanoimprint technique the mold (in this case elastomeric) is placed on to the methacryl silica–titania hybrimer film. The PDMS mold was then pressed flat with pressure during the UV curing process. Because the methacryl silica–titania can be cured with small quantity of UV energy (2–3 J cm^{-2}), 30 s of irradiation by UV light (365 nm, 80 mW) is enough to fabricate a photonic crystal pattern onto methacryl silica–titania film. Because the volume shrinkage of methacryl silica–titania hybrimer between before and after UV curing shows low enough as 2–2.5 vol% measured by Archimedes methods, the imprinted photonic crystal is a same counterpart of the original master. In Fig. 4(C), the UV-based nanoimprinted circular holes of methacryl silica–titania hybrimer appear to conform to the PDMS mold and the original silicon master. The dark centers of the holes correspond to the nanoimprint of the narrow shafts of the rods on the PDMS mold. Holes having 105 nm diameter, 408 nm pitch, and 127 nm depth were obtained with the PDMS mold by the UV-based nanoimprint technique.

Conclusions

High refractive index organic–inorganic hybrid materials (hybrimers) for photonic crystal nanostructures were successfully synthesized by a non-hydrolytic sol–gel process. This hybrimer has low absorption loss and is very well polycondensed. Nanoimprinting with the UV-based technique was employed to fabricate a hybrimer thin film with photonic crystal nanostructures. Thus, the UV-based nanoimprint technique is an efficient method to fabricate polymeric photonic crystal nanostructures, which is undoubtedly a very promising route for optics technologies. Experimental work to fabricate photonic crystal devices is currently under way. We will report on the optical properties of photonic crystal waveguides in the near future.

Acknowledgements

This work is supported by the Sol–Gel Innovation Project (SOLIP) of the Ministry of Commerce, Industry and Energy of Korea.

References

1 E. Yablonovitch, *Phys. Rev. Lett.*, 1987, **58**, 2059–2062.
2 S. Fan, P. R. Villeneuve, J. D. Joannopoulos and E. F. Schubert, *Phys. Rev. Lett.*, 1997, **78**, 3294–3297.
3 H. Kosaka, T. Kawashima, A. Tomina, M. Notomi, T. Tamamura, T. Sato and S. Kawakami, *Phys. Rev. B: Condens. Matter*, 1998, **58**, 10096–10099.
4 L. Wu, M. Mazilu and T. F. Krauss, *J. Lightwave Technol.*, 2003, **21**, 561–566.
5 X. Yu and S. Fan, *Appl. Phys. Lett.*, 2003, **83**, 3251–3253.
6 P. Halevi, A. A. Krokhin and J. Arriaga, *Phys. Rev. Lett.*, 1999, **82**, 719–722.
7 J. D. Joannopoulos, P. R. Villeneuve and S. Fan, *Nature*, 1997, **386**, 143–149.
8 A. Birner, R. B. Wehrspohn, U. M. Gösele and K. Busch, *Adv. Mater.*, 2001, **13**, 377–388.
9 C. López, *Adv. Mater.*, 2003, **15**, 1679–1704.
10 S. Y. Chou, P. R. Krauss and P. J. Resnstrom, *Appl. Phys. Lett.*, 1995, **67**, 3114–3116.
11 Y. Xia, J. A. Rogers, K. E. Paul and G. M. Whitesides, *Chem. Rev*, 1999, **99**, 1823–1848.
12 S. Y. Chou, P. R. Krauss, W. Zhang, L. Guo and L. Zhuang, *J. Vac. Sci. Technol., A*, 1997, **15**, 2897–2904.
13 J. Haisma, M. Verheijen, K. v. d. Heuvel and J. v. d. Berg, *J. Vac. Sci. Technol., B*, 1996, **14**, 4124–4128.
14 M. Bender, M. Otto, B. Vratzov, B. Spengenberg and H. Kurz, *Microelectron. Eng.*, 2000, **53**, 233–236.
15 Z. Yu, P. Deshpande, W. Wu, J. Wang and S. Y. Chou, *Appl. Phys. Lett.*, 2000, **77**, 927–929.
16 M. Nagawa, M. Ichikawa, T. Koyama, H. Shirai, T. Taniguchi, A. Hongo, S. Tsuhi and Y. Nakano, *Appl. Phys. Lett.*, 2000, **77**, 2641–2643.
17 C. Liguda, G. Böttger, A. Kuligk, R. Blum, M. Eich, H. Roth, J. Kunert, W. Morgenroth, H. Elsner and H. G. Meyer, *Appl. Phys. Lett.*, 2001, **78**, 2434–2436.
18 J. Seekamp, S. Zankovych, A. H. Helfer, P. Maury, C. M. Sotomayor Torres, G. Böttger, C. Liguda, M. Eich, B. Heidari, L. Montelius and J. Ahopelto, *Nanotechnology*, 2002, **13**, 581–586.
19 C. M. Sotomayor Torres, S. Zankovych, J. Seekamp, A. P. Kam, C. Clavijo Cedeño, T. Hoffmann, J. Ahopelto, F. Reuther, K. Pfeiffer, G. Bleidiessel, G. Gruetzner, M. V. Maximov and B. Heidari, *Mater. Sci. Eng., C*, 2003, **23**, 23–31.
20 B. S. Bae, *J. Sol–Gel Sci. Technol.*, 2004, **31**, 309–315.
21 W. S. Kim, K. S. Kim, Y. J. Eo, K. B. Yoon and B. S. Bae, *J. Mater. Chem.*, 2005, **15**, 465–469.
22 W. S. Kim, J. H. Lee, S. Y. Shin, B. S. Bae and Y. C. Kim, *IEEE Photon. Technol. Lett.*, 2004, **16**, 1888–1890.
23 C. C. Chang and W. C. Chen, *J. Polym. Sci., Polym. Chem. Ed*, 2001, **39**, 3419–3427.
24 K. B. Yoon, C.-G. Choi and S.-P. Han, *Jpn. J. Appl. Phys.*, 2004, **43**, 3450–3451.
25 J. T. Kim, K. B. Yoon and C.-G. Choi, *IEEE Photon. Technol. Lett.*, 2004, **16**, 1664–1666.